Magnetic Resonance Imaging 63 (2019) 131–136

Contents lists available at ScienceDirect

Magnetic Resonance Imaging

journal homepage: www.elsevier.com/locate/mri

Original contribution

Diffusion kurtosis imaging as an imaging biomarker for predicting prognosis of the patients with high-grade gliomas

Xiao Wang[a], Wenjing Gao[b], Fuyan Li[c], Wenqi Shi[d], Hongxia Li[e], Qingshi Zeng[f,*]

[a] Department of Radiology, Jining No.1 People's Hospital, Jining, China
[b] Department of CT/MRI, ZiBo Central Hosipital, Zibo, China
[c] Department of Radiology, Shandong Medical Imaging Research Institute, Jinan, China
[d] The Third Affiliated Hospital of Sun Yat-sen University, Guangzhou, China
[e] Department of Radiology, The Second Hospital of Shandong University, Jinan, China
[f] Department of Radiology, Qilu Hospital of Shandong University, Jinan, China

A B S T R A C T

Purpose: To retrospectively explore the utilization of MR diffusion kurtosis imaging (DKI) in predicting prognosis of the patients with high-grade gliomas.

Materials and methods: Thirty-three consecutive patients with cerebral gliomas underwent pretreatment DKI and diffusion-weighted imaging examination on a 3.0-T MR scanner. Diffusion parameters, including conventional tensor parameters, kurtosis metrics (mean kurtosis [MK], radial kurtosis [AK], and axial kurtosis [RK]), and minimum apparent diffusion coefficient (minADC), were obtained and normalized to the contralateral normal-appearing white matter. Correlations among each diffusion parameter and overall survival were analyzed by a Spearman method. The diagnostic efficiency of each parameter in predicting survival for patients with high-grade gliomas was assessed by a receiver operating characteristic curve. The favorable prognostic imaging biomarkers were further analyzed by using a Kaplan-Meier method with log-rank test.

Results: In 33 patients, 17 patients reached overall survival > 15 months (long survival group), whereas 16 showed overall survival < 15 months (short survival group). Negative correlations between kurtosis metrics (MK, AK, and RK) and overall survival were obtained by using Spearman analysis ($r = -0.63$, -0.57, and -0.61, respectively, all $P < 0.01$), whereas minADC was positively correlated with overall survival ($r = 0.56$, $P < 0.01$). The kurtosis parameters of the long survival group were significantly lower than that of the short survival group ($P < 0.001$), while the minADC of the long survival group was significantly higher than that of the short survival group ($P = 0.002$). Among these diffusion parameters, the optimal cut-off value of MK (0.688) provided the best combination of sensitivity (93.75%) and specificity (76.47%) for differentiation of patients with long survival from those with short survival. High kurtosis metrics and low minADC were significant predictors of poor outcome. ($P < 0.05$).

Conclusion: Both kurtosis metrics and minADC have the potential to predict survival for the patients with high-grade gliomas. The preoperative kurtosis parameters, especially MK, can be taken as a preoperative prognostic biomarker to predict prognosis in patients with high-grade gliomas.

1. Introduction

According to the 2007 WHO tumor classification of the central nervous system, gliomas are divided into four grades depending on their histological phenotype [1]. High-grade gliomas, including WHO grades III (anaplastic astrocytoma) and IV (glioblastomas multiforme), are characterized with high morbidity and low survival rates [2]. The WHO classification of gliomas is a strong prognostic factor. Patients exhibit the same histopathologic diagnosis and undertake a uniform postoperative treatment; however, the response to therapy and prognosis of individual patient is relatively variable. Except for pathological diagnosis, many factors, such as age, tumor localization, and necrosis [3,4], can result in the prognostic difference, but the most notable point is the high tumor heterogeneity caused by different histomorphologies and molecular features [4]. Therefore, precise analysis of heterogeneity may contribute to evaluating the prognosis of patients with high-grade gliomas.

Conventional diffusion imaging, including diffusion-weighted imaging (DWI) and diffusion tensor imaging (DTI), have been used to reflect tissue microstructural changes in brain tissue [5–8]. These imaging techniques are based on the simplified premise of the Gaussian distribution of water diffusion in biological systems. In addition, the reality, that complex intracellular and extracellular in vivo environments cause the diffusion of water molecules to deviate considerably from this pattern, is ignored [9]. Thus, this deviation results in an inaccurate reflection of tissue microstructure [10,11].

Diffusional kurtosis imaging (DKI), an advanced diffusion imaging model, has been increasingly implemented for providing more precise

* Corresponding author at: Department of Radiology, Qilu Hospital of Shandong University, 107 Wenhuaxi Road, Jinan 250012, Shandong Province, China.
E-mail address: zengqingshi@gmail.com (Q. Zeng).

https://doi.org/10.1016/j.mri.2019.08.001
Received 16 February 2019; Received in revised form 8 July 2019; Accepted 15 August 2019
0730-725X/

information of tissue characteristics based on quantifying non-Gaussian behavior of water molecules in brain tissue [12]. With DKI, all the DTI tensor parameters, such as the mean diffusivity (MD) and fractional anisotropy (FA), can be obtained, and several kurtosis metrics, such as mean kurtosis (MK), axial kurtosis (AK), and radial kurtosis (RK), can be also evaluated. Given the high sensitivity and specificity of DKI in assessing tissue microstructure [12–15], the present study aimed to *(1)* investigate the utilization of kurtosis parameters in evaluating the prognosis of patients with high-grade gliomas, and *(2)* further explore whether kurtosis parameters were more accurate than conventional diffusion parameters in evaluating prognosis.

2. Material and methods

2.1. Inclusion criteria for patients

The institutional review board approved this study and all patients voluntarily signed informed consent. We retrospectively analyzed 36 patients who underwent DKI examination preoperatively for suspected supratentorial gliomas between September 2014 and December 2015.

The patients enrolled in this clinical study must satisfy the following criteria: (1) a complete MRI data containing a routine magnetic resonance sequence, DWI, and DKI within 2 weeks before surgery; (2) no other previous malignant systemic disease and intracranial surgery; (3) histopathological diagnosis of cerebral gliomas by subsequent surgical resection; and (4) available contact information at the time of follow-up. We excluded two patients who were preoperatively suspected of supratentorial gliomas but pathologically confirmed as a solitary metastasis after resection and a patient who withdrew at the time of follow-up.

According to the National Comprehensive Cancer Network (NCCN) guidelines and the treatment protocol of our hospital, surgical removal was undertaken in all patients. After surgery, the patients received radiotherapy and chemotherapy.

Tissue samples obtained by surgical resection were examined histopathologically by an experienced neuropathologist (with 8 years of experience in diagnosis of gliomas). Glioma grading was based on the WHO classification system [1].

2.2. Imaging acquisition

All preoperative magnetic resonance scanning procedures were performed on a 3.0-T MR scanner (Verio, Siemens, Germany) with an eight-channel head coil for signal reception.

The DWI protocol was as follows: a single-shot spin-echo echoplanar imaging sequence program with two b-values (0 and 1000 s/mm^2), field of view = 256 mm × 256 mm, acquisition matrix = 128 × 128, slice number = 20, section thickness of 5 mm, TE = 100 ms, TR = 4500 ms, and average = 1. The total acquisition time for the protocol was 33 s.

DKI data were acquired in an ep2d_diff sequence through the following protocol: axial plane with six b values (0, 500, 1000, 1500, 2000, and 2500 s/mm^2), with every b value encoded with 30 diffusion directions; field of view = 256 mm × 256 mm, acquisition matrix = 128 × 128, slice number = 15, section thickness = 4 mm, TE = 109 ms, TR = 3000 ms, and average = 2. The total acquisition time for this protocol was 15 min and 17 s.

The following acquisition parameters of plain scan and contrast-enhanced (CE) sequences were applied: TR = 4000 ms, TE = 93 ms, field of view = 256 mm × 256 mm, matrix = 320 × 224 for plain transverse T2-weighted turbo spin echo imaging (T2WI) sequence; TR = 250 ms, TE = 2.48 ms, field of view = 256 mm × 256 mm, and matrix = 256 × 256 for the CE transverse T1-weighted fast-spin echo imaging (CE-T1WI) sequence. The section thickness and slice number of the two sequences were 5 mm and 20 slices, respectively.

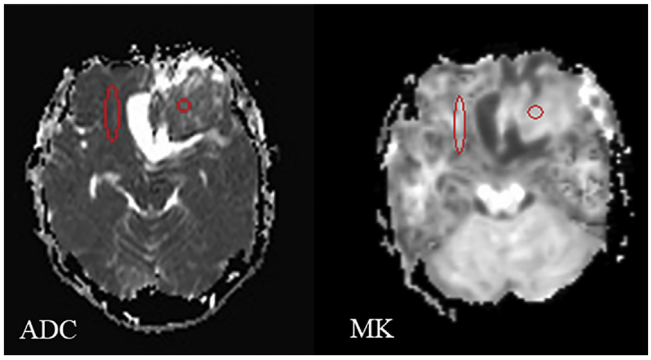

Fig. 1. Delineation of ROIs.
For the ADC value, we selected the low signal areas of ADC maps and manually placed five to ten round-shaped ROIs(area, approximately 0.3–0.5 cm^2)on the ADC maps individually, the lowest ADC value was selected as the minimum ADC value (minADC). For the DKI parameters, the ROIs were delineated on the region of the above mentioned ROI which have the lowest ADC value.

2.3. Data processing and delineating regions of interest (ROIs)

On the basis of the DWI images, an apparent diffusion coefficient (ADC) map was automatically generated according to the formula ADC = (ln(Sb/S0))/b at the Siemens Syngo workstation. The DKI data were processed using the Diffusional Kurtosis Estimator (DKE 2.6, http://www.nitrc.org/projects/dke). Tensor parameters (MD and FA) and kurtosis metrics (MK, AK, and RK) were obtained.

Details of the postprocessing procedure for DWI and DKI have been reported previously [14,15]. In brief, ROIs were manually drawn on ADC and DKI parameter maps by two neuroradiologists respectively (each radiologist perform one set of data), who were blinded to the patients' histopathological results, as presented in Fig. 1. Before delineating the ROIs, FMRIB's diffusion toolbox (FSL 4.0, http://www.fmrib.ox.ac.uk/fsl) was used to correct the eddy current-induced distortion and the slightly image variation. MATLAB 8.2 (Mathworks, Natick, MA, USA) and SPM8 software (http://www.fil.ion.ucl.ac.uk/spm/software/) were used to coregister and reslice the DKI parameter maps and match with the original reference images.

For the ADC value, we selected the low signal areas of ADC maps and manually placed five to ten round-shaped ROIs(area, approximately 0.3–0.5 cm^2)on the ADC maps individually at the Siemens Syngo workstation. Finally, the lowest ADC value was selected as the minimum ADC value (minADC). For the DKI parameters, the ROIs were delineated on the region of the above mentioned ROI which have the lowest ADC value. Subsequently, the ROIs were copied to each DKI parameter map to calculate the tensors and kurtosis values by using MRIcro software (http://www.cabiatl.com/mricro/mricro/mricro.html). The above-mentioned methods of drawing ROIs were conducted carefully to avoid the necrotic and hemorrhagic tumor areas. Meanwhile, the tensor parameters, kurtosis metrics, and minADC values in the contralateral normal-appearing white matter (NAWM) were obtained.

2.4. Statistical analysis

SPSS Statistics 19.0 (IBM Corp. Armonk, NY, USA) and MedCalc16.7 software (MedCalc statistical software, Ostend, Belgium) were used for statistical data analysis. Differences with P values < 0.05 were considered statistically significant. To examine the test–retest reliability of quantitative data, two sets of measurement data analyzed by radiologists were evaluated by using the intraclass correlation coefficient (ICC).

To evaluate the potential of minADC, MD, FA, MK, AK, and RK values in predicting patient's post-operative overall survival,

Table 1
DKI and DWI diffusion parameters in solid part of glioma and NAWM.

Parameter	Number	MK	AK	RK	FA	MD (10^{-3} mm^2/s)	minADC (10^{-3} mm^2/s)
NAWM	33	1.031 ± 0.086	0.799 ± 0.047	1.226 ± 0.143	0.382 ± 0.075	0.943 ± 0.067	0.759 ± 0.021
Grade III	11	0.631 ± 0.092	0.593 ± 0.096	0.663 ± 0.101	0.154 ± 0.042	1.314 ± 0.179	0.987 ± 0.151
Grade IV	22	0.777 ± 0.066	0.731 ± 0.073	0.790 ± 0.078	0.142 ± 0.036	1.278 ± 0.246	0.825 ± 0.122
HGGs	33	0.728 ± 0.102	0.684 ± 0.103	0.748 ± 0.104	0.146 ± 0.038	1.290 ± 0.224	0.879 ± 0.151

Note—Values are the mean ± standard deviation.
DKI: diffusion kurtosis imaging; DWI: diffusion-weighted imaging; NAWM: contralateral normal-appearing white matter; MK: mean kurtosis; RK: radial kurtosis; AK: axial kurtosis; MD: mean diffusivity; FA: fractional anisotropy; minADC: minimum apparent diffusion coefficient; HGGs: high-grade gliomas including grade III and grade IV.

Table 2
DKI and DWI diffusion parameters normalized to the NAWM in solid part of glioma.

Parameter	Number	N-MK	N-AK	N-RK	N-FA	N-MD (10^{-3} mm^2/s)	N-minADC (10^{-3} mm^2/s)
Grade III	11	0.609 ± 0.096	0.734 ± 0.133	0.535 ± 0.087	0.412 ± 0.177	1.459 ± 0.240	1.300 ± 0.207
Grade IV	22	0.760 ± 0.076	0.925 ± 0.120	0.660 ± 0.108	0.388 ± 0.101	1.342 ± 0.304	1.089 ± 0.169
HGGs	33	0.709 ± 0.109	0.862 ± 0.153	0.618 ± 0.116	0.396 ± 0.129	1.381 ± 0.286	1.159 ± 0.205

Note. Values are the mean ± standard deviation.
NAWM: contralateral normal-appearing white matter. N-MK, N-RK, N-AK, N-FA, N-MD, and N-minADC: mean kurtosis, radial kurtosis, axial kurtosis, fractional anisotropy, mean diffusivity, and minimum apparent diffusion coefficient normalized to the contralateral normal-appearing white matter, respectively.

Table 3
ICCs of two sets of measurement data in solid part of glioma and NAWM.

Tumor	MK	AK	RK	FA	MD	ADC
ICC	0.977	0.968	0.976	0.908	0.912	0.950
(95%CI)	(0.953–0.989)	(0.934–0.984)	(0.952–0.988)	(0.818–0.953)	(0.828–0.956)	(0.902–0.974)
NAWM	MK_{NAWM}	AK_{NAWM}	RK_{NAWM}	FA_{NAWM}	MD_{NAWM}	ADC_{NAWM}
ICC	0.940	0.937	0.918	0.907	0.933	0.874
(95%CI)	(0.884–0.969)	(0.878–0.968)	(0.840–0.958)	(0.819–0.952)	(0.870–0.965)	(0.755–0.935)

Note—CI: confidence interval;
ICCs: intraclass correlation coefficients; NAWM: contralateral normal-appearing white matter; MK: mean kurtosis; RK: radial kurtosis; AK: axial kurtosis; MD: mean diffusivity; FA: fractional anisotropy; ADC: apparent diffusion coefficient.

Table 4
Differences in age, survival and diffusion parameters between LS group† and SS group†.

Parameter	LS group (n = 17)	SS group (n = 16)	P value
Age (years)	49.24 ± 8.07	55.19 ± 10.53	0.114✖
Survival (months)	22.27 ± 4.32	10.81 ± 3.57	< 0.001
N-MK	0.636 ± 0.088	0.788 ± 0.066	< 0.001
N-AK	0.771 ± 0.119	0.958 ± 0.124	< 0.001
N-RK	0.551 ± 0.083	0.690 ± 0.104	< 0.001
N-FA	0.385 ± 0.093	0.407 ± 0.161	0.63✖
N-MD	1.450 ± 0.247	1.307 ± 0.314	0.15✖
N-minADC	1.262 ± 0.187	1.050 ± 0.167	0.002

Note. Values are the mean ± standard deviation.
† LS group: survival time over 15-months (long survival group), SS group: survival time less15-months (short survival group).
✖ no significant difference .
N-MK, N-RK, N-AK, N-FA, N-MD, and N-minADC: mean kurtosis, radial kurtosis, axial kurtosis, fractional anisotropy, mean diffusivity, and minimum apparent diffusion coefficient normalized to the contralateral normal-appearing white matter, respectively.

independent samples *t*-test was used to compare the differences of the diffusion parameters between two groups (over 15 months: long survival group, or less 15 months: short survival group). Receiver operating characteristic (ROC) curves were utilized to characterize each parameter value for evaluating the overall survival of high-grade gliomas. The area under the ROC curve (AUC) was calculated, and the highest value was selected to determine the optimal cut-off value, and then the patients were grouped again by these optimal cut-off values to draw a Kaplan-Meier survival curves, and the differences of survival between the two groups were obtained. Prognostic value of parameters was performed using Cox regression analysis.

The Z test was used to compare the differences in AUC among minADC, MD, FA, MK, AK, and RK values. The correlations among each diffusion parameter value and overall survival were analyzed by Spearman correlation analysis.

3. Results

3.1. Patients

A total of 33 patients with glioma included 16 females and 17 males aged between 29 years and 67 years (mean age ± standard deviation: 52.21 ± 9.36 years). These patients included 11 WHO grade III anaplastic astrocytomas, and 22 WHO grade IV glioblastomas. We classified patients with high-grade glioma into two groups with respect to the 15-month survival; this classification was adopted because a previous research shows that 15 months is the median postoperative survival in patients with high-grade glioma [2]. The patients with high-grade gliomas were followed up by telephone in a unified time period. Overall survival was calculated from the time of surgery to death or the date of follow-up. The range of overall survival was 3.5–30 months, with mean time ± standard deviation of 16.7 ± 7.0 months.

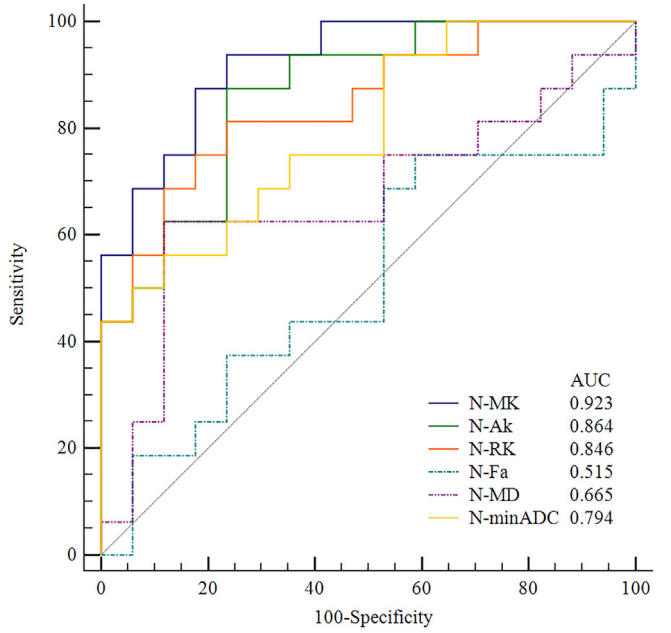

Fig. 2. ROC curves of diffusion parameters in the solid tumor part for predicting the 15-month survival of patients with high-grade gliomas.
N-MK achieved the higher AUC (0.923); however, N-FA and N-MD showed lower values with AUCs of 0.515 and 0.665, respectively.
AUC: area under the ROC curve; N-MK, N-AK, N-RK, N-FA, N-MD, and N-minADC: mean kurtosis, axial kurtosis, radial kurtosis, fractional anisotropy, mean diffusivity, and minimum apparent diffusion coefficient normalized to the contralateral normal-appearing white matter, respectively.

3.2. Normalization of MRI data to facilitate interpatient comparisons

The tensor parameters, kurtosis metrics, and minADC values in the tumor and NAWM are shown in Table 1. DKI and DWI diffusion parameters normalized to the NAWM in solid part of glioma are shown in Table 2. The ICC values of the two sets of measurement data, including MD, FA, MK, AK, RK, and minADC, in the solid part of tumor and those in the contralateral NAWM (except the ICC in NAWM of ADC was above 0.8) were above or equal to 0.9, as presented in Table 3.

Previous study shows that the MK, RK, and FA in the NAWM decrease with aging, whereas the MD increases [16]. To eliminate the minor differences caused by age and tumor location, we selected normalized data as the final research parameters, that is, all diffusion parameters were normalized to the contralateral NAWM. Hereinafter, the parameters were referred to as the N-MK, N-AK, N-RK, N-FA, N-MD and N-minADC.

3.3. N-MK: An optimal parameter for predicting the 15-month survival of high-grade gliomas

Among all the 33 patients with high-grade glioma, 17 reached overall survival > 15 months (long survival group), whereas 16 showed overall survival < 15 months (short survival group). Negative correlations between diffusion parameters (N-MK, N-AK, and N-RK) and overall survival were determined by using Spearman analysis ($r = -0.63$, -0.57, and -0.61, respectively, all $P < 0.01$), whereas N-minADC was positively correlated with overall survival ($r = 0.56$, $P < 0.01$). We found no correlation for N-FA and N-MD with overall survival, respectively ($P > 0.05$).

Except for age, N-FA, and N-MD, the remaining parameters were statistically different between the two groups (Table 4). N-MK, N-AK, and N-RK were evidently lower in the long survival group than those in the short survival group ($P < 0.001$), whereas N-minADC was higher in the long survival group than that in the short survival group ($P = 0.002$).

The ROC curves of each parameter in predicting the 15-month survival of the two groups are presented in Fig. 2. N-MK (0.923), N-AK (0.864), N-RK (0.846), and N-minADC (0.794) achieved the highest AUC sequentially. However, N-FA and N-MD showed lower values with AUCs of 0.515 and 0.665, respectively. The AUC of N-MK was significantly higher than those of N-FA and N-MD ($P < 0.01$).

When N-MK, N-AK, N-RK, and N-minADC were selected as the predictive parameters of survival, their optimal cut-off values (with the most remarkable combination of sensitivity and specificity: the maximal Youden index) were 0.688 (93.75% and 76.47%), 0.825 (87.50% and 76.47%), 0.588 (81.25% and 76.47%), and 1.159 (75.00% and 64.71%), respectively. When the prognosis was compared between the two groups divided by using the above cut-off value and the Kaplan–Meier survival curve, the group with high N-MK, N-AK, N-RK and low N-minADC predicted significantly poor outcome ($P < 0.05$) (Fig. 3).

We used Cox regression analysis to assess the effect of the parameters (necrosis, two or more lobes were involved, tumor grade, N-MK and N-minADC) on patient overall survival. The results showed that except for N-MK and N-minADC, the remaining variables have no statistically significant effect on patient's overall survival (Table 5).

4. Discussion

Gliomas, one of the most common types of primary brain tumors, can affect patient's brain function and be life-threatening. Despite improvements in surgical resection, radiotherapy, and chemotherapy, the prognosis remains poor in patients with high-grade gliomas [2]. To our knowledge, few groups conducted studies investigating whether preoperative DKI metrics can effectively evaluate prognosis of post-treatment outcome in patients with high-grade gliomas [17,18]. In the present study, our results revealed that both kurtosis parameters and minADC have the potential to predict survival for the patients with high-grade gliomas. Furthermore, the preoperative kurtosis parameters, especially MK value, showed a higher sensitivity and specificity than those of conventional diffusion parameters for evaluating prognosis, and the patient with high kurtosis metrics and low minADC predicted significantly poor outcome.

Gliomas, especially for high-grade gliomas, are characterized by increased microstructural complexity and heterogeneity. Previous study shows DWI and DTI have been utilized for the evaluation of microstructure and tumor cellularity [19]. However, tissue complexity, such as cell membranes, organelles, and water compartments, cause compartmentalization and restrict the free displacement of water molecules, which lead to a non-Gaussian diffusion of water [20]. Thus, due to complex tissue microstructure, these imaging technologies may have limitations for assessing the glioma heterogeneity [10,11]. DKI, as an advanced non-Gaussian diffusion imaging technique, provides a more accurate model of diffusion for quantifying diffusion kurtosis metrics to account for this deficiency [20]. By data acquisition for at least two nonzero diffusion gradient factors (b value) in > 15 nonlinear directions, the kurtosis metrics (including MK, AK and RK) and diffusion metrics (including MD and FA) are obtained simultaneously. AK and RK are designed to specifically address direction-dependent tissue complexity. AK, parallel to the main direction of diffusion, might reflect the axonal integrity and density of fiber bundles. RK, perpendicular to the main direction of diffusion, might reflect the myelin integrity and axonal density. The MK is defined as the average kurtosis over all diffusion directions. MK is not only limited to anisotropic environment, but also can uniquely quantify the microstructural integrity of brain tissue, even in the presence of cross-fibers [21,22]. Previous study confirmed that DKI, as an extension of DTI, can be generally proportional to the heterogeneity and complexity of the microstructure [21,23]. In addition, higher grade gliomas are characterized by higher cellularity, more nuclear atypia, higher pleomorphism and heterogeneity with vascular

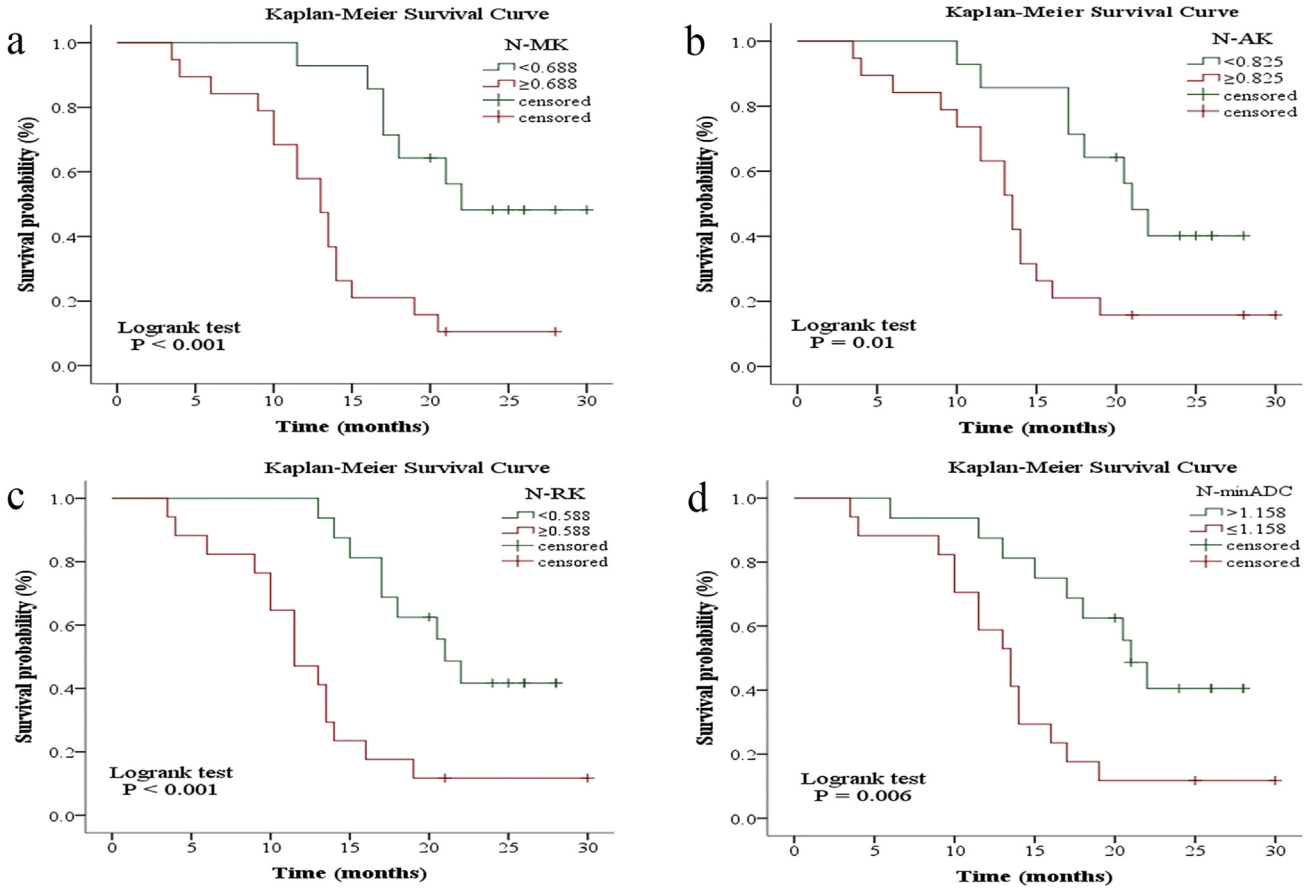

Fig. 3. Kaplan–Meier survival curve for patient with high-grade gliomas. Figure (a–d) presents the Kaplan–Meier survival curve of N-MK, N-AK, N-RK, and N-minADC, respectively. Patients with high kurtosis parameter values (a, b, and c) and low minADC (d) values achieve significantly poor outcomes.
N-MK, N-AK, N-RK, and N-minADC: mean kurtosis, axial kurtosis, radial kurtosis, and minimum apparent diffusion coefficient normalized to the contralateral normal-appearing white matter, respectively.

Table 5
Survival analyses using cox regression.

Parameters	n	*P* value
Grade		> 0.05
Grade III	11	
Grade IV	22	
Necrosis		> 0.05
Yes	19	
No	14	
Location(two or more lobes involved)		> 0.05
Yes	10	
No	23	
N-MK		0.01
< 0.688	14	
≥ 0.688	19	
N-minADC		0.049
> 1.158	16	
≤ 1.158	17	

hyperplasia, necrosis, hemorrhage, and endothelial proliferation. Therefore, higher grade gliomas contain greater structural complexity and heterogeneity [14,19,21]. Hence, increased values of kurtosis parameters in high-grade glioma might reflect a higher degree of tissue complexity, and these changes can be the reason why the kurtosis metrics had correlations with overall survival and the patient with the high kurtosis parameter values implied a significantly poor outcome.

The preoperative minADC, as a useful clinical prognostic biomarker for survival in patients with high-grade gliomas, was reported in the previous researches [6,7]. The minADC was selected as a prognostic value because the area with minADC indicates the most aggressive part of the tumor with high proliferation and cellularity [24–26]. Thus, in the present study, we selected an area with minADC as ROIs. Our study further revealed that the AUC of MK parameter was higher than that of the minADC for predicting the 15-month survival. This result may be attributed to the following reasons. On one hand, a previous study revealed that tumor cellularity showed strong positive correlation with microvascular density, while high tumor cellularity can decrease ADC value [26]. The high microvascular density may increase the ADC, since ADC value is calculated from the monoexponential model incorporating both diffusion and perfusion information of the tumor tissue. On the other hand, the diffusion of water molecules of microstructures in vivo is much closer to non-Gaussian distribution [9]. Therefore, ADC value obtained from DWI, which is based on the monoexponential and idealized Gaussian distribution model, may not be able to accurately reflect water molecular diffusion in such complex microenvironment. In addition, DKI can depict the non-Gaussian diffusion behavior and reflect the deviation degree of Gaussian diffusion of water molecules movement. This imaging technique is able to reveal microstructural changes within glioma tissue, and a large diffusional kurtosis suggests a high degree of diffusional heterogeneity and microstructural complexity [12,14,27]. Furthermore, by using Cox regression analysis, prognostic value of parameters (tumor localization, grade and necrosis) was different from previous studies [3,4], which may be account for the fact that the sample size of the present study was not large. However, the results may be further confirmed the accuracy of N-MK to assess the

overall survival of patients in our data.

Our study also exhibited some limitations. First, given our study's retrospective design, the most aggressive area of glioma may not correspond with the delineated ROIs. However, previous researches revealed that the ROIs with reference of intensely enhancement indicate the solid tumor part. (The obviously enhancement area represents the substantial part of the tumor and also indicates the active part of the tumor growth, [14,15] we chose this area as the ROI, which can make up for the above deficiency). Second, the sample size of the present study was not large. Further study should expand the sample size and confirm that DKI can reflect the heterogeneity of high-grade gliomas and evaluate its correlation with patient prognosis comprehensively. Finally, the study included patients with histopathology identified as anaplastic astrocytoma and glioblastoma according to the 2007 WHO classification instead of 2016 version.

5. Conclusions

The preoperative kurtosis metrics in patients with high-grade gliomas, especially MK values, demonstrate a significantly higher sensitivity and specificity than those of the conventional diffusion values in evaluating tumor prognosis. The glioma patients with the high kurtosis parameters show poor outcomes. Therefore, the kurtosis metrics, as a preoperative prognostic biomarker, can predict prognosis in patients with high-grade gliomas.

Acknowledgement

The study was supported by the National Natural Science Foundation of China, contract grant numbers: 81372439 and 81771939.

References

[1] Louis DN, Perry A, Reifenberger G, Deimling AV, Figarellabranger D, Cavenee WK, et al. The 2016 World Health Organization classification of tumors of the central nervous system: a summary. Acta Neuropathol 2016;131(6):803–20.
[2] Jiang T, Mao Y, Ma W, Mao Q, You Y, Yang X, et al. CGCG clinical practice guidelines for the management of adult diffuse gliomas. Cancer Lett 2016;375(2):263–73.
[3] Helseth R, Helseth E, Johannesen TB, Langberg CW, Lote K, Rønning P, et al. Overall survival, prognostic factors, and repeated surgery in a consecutive series of 516 patients with glioblastoma multiforme. Acta Neurol Scand 2010;122(3):159–67.
[4] Homma T, Fukushima T, Vaccarella S, Yonekawa Y, Di Patre PL, Franceschi S, et al. Correlation among pathology, genotype, and patient outcomes in glioblastoma. Neuropathol Exp Neurol 2006;65(9):846–54.
[5] Murakami R, Hirai T, Kitajima M, Fukuoka H, Toya R, Nakamura H, et al. Magnetic resonance imaging of pilocytic astrocytomas: usefulness of the minimum apparent diffusion coefficient (ADC) value for differentiation from high-grade gliomas. Acta Radiol 2008;49(4):462–7.
[6] Murakami R, Sugahara T, Nakamura H, Hirai T, Kitajima M, Hayashida Y, et al. Malignant supratentorial astrocytoma treated with postoperative radiation therapy: prognostic value of pretreatment quantitative diffusion-weighted MR imaging. Radiology 2007;243(2):493–9.
[7] Higano S, Yun X, Kumabe T, Watanabe M, Mugikura S, Umetsu A, et al. Malignant astrocytic tumors: clinical importance of apparent diffusion coefficient in prediction of grade and prognosis. Radiology 2006;241(3):839–46.
[8] Qu J, Qin L, Cheng S, Leung K, Li X, Li H, et al. Residual low ADC and high FA at the resection margin correlate with poor chemoradiation response and overall survival in high-grade glioma patients. Eur J Radiol 2016;85(3):657–64.
[9] Steven AJ, Zhuo J, Melhem ER. Diffusion kurtosis imaging: an emerging technique for evaluating the microstructural environment of the brain. AJR Am J Roentgenol 2014;202(1):26–33.
[10] Lam WW, Poon WS, Metreweli C. Diffusion MR imaging in glioma: does it have any role in the pre-operation determination of grading of glioma? Clin Radiol 2002;57(3):219–25.
[11] Lee H, Na D, Song I, Lee D, Seo H, Kim J, et al. Diffusion-tensor imaging for glioma grading at 3-T magnetic resonance imaging: analysis of fractional anisotropy and mean diffusivity. Comput Assist Tomogr 2015;32(2):298–303.
[12] Wu EX, Cheung MM. MR diffusion kurtosis imaging for neural tissue characterization. NMR Biomed 2010;23(7):836–48.
[13] Sauwen N, Sima DM, Van Cauter S, Veraart J, Leemans A, Maes F, et al. Hierarchical non-negative matrix factorization to characterize brain tumor heterogeneity using multi-parametric MRI. NMR Biomed 2015;28(12):1599–624.
[14] Raab P, Hattingen EK, Zanella FE, Lanfermann H. Cerebral gliomas: diffusional kurtosis imaging analysis of microstructural differences. Radiology 2010;254(3):876–81.
[15] Van Cauter S, Veraart J, Sijbers J, Peeters RR, Himmelreich U, De Keyzer F, et al. Gliomas: diffusion kurtosis MR imaging in grading. Radiology 2012;263(2):492–501.
[16] Falangola MF, Jensen JH, Babb JS, Hu C, Castellanos FX, Martino AD, et al. Age-related non-Gaussian diffusion patterns in the prefrontal brain. Magn Reson Imaging 2008;28(6):1345–50.
[17] Hempel JM, Brendle C, Bender B, Bier G, Kraus MS, Skardelly M, et al. Diffusion kurtosis imaging histogram parameter metrics predicting survival in integrated molecular subtypes of diffuse glioma: an observational cohort study. Eur J Radiol 2019;112:144–52.
[18] Chakhoyan A, Woodworth DC, Harris RJ, Lai A, Nghiemphu PL, Liau LM, et al. Mono-exponential, diffusion kurtosis and stretched exponential diffusion MR imaging response to chemoradiation in newly diagnosed glioblastoma. J Neurooncol 2018;139(3):651–9.
[19] Qi C, Yang S, Meng L, Chen H, Li Z, Wang S, et al. Evaluation of cerebral glioma using 3T diffusion kurtosis tensor imaging and the relationship between diffusion kurtosis metrics and tumor cellularity. Int Med Res 2017;45(4):1347–58.
[20] Jensen JH, Helpern JA, Ramani A, Lu H, Kaczynski K. Diffusional kurtosis imaging: the quantification of non-gaussian water diffusion by means of magnetic resonance imaging. Magn Reson Med 2005;53(6):1432–40.
[21] Jiang R, Jiang J, Zhao L, Zhang J, Zhang S, Yao Y, et al. Diffusion kurtosis imaging can efficiently assess the glioma grade and cellular proliferation. Oncotarget 2015;6(39):42380–93.
[22] Helpern JA, Adisetiyo V, Falangola MF, Hu C, Di Martino A, Williams K, et al. Preliminary evidence of altered gray and white matter microstructural development in the frontal lobe of adolescents with attention-deficit hyperactivity disorder: a diffusional kurtosis imaging study. Magn Reson Imaging 2011;33(1):17–23.
[23] Tietze A, Hansen MB, Ostergaard L, Jespersen SN, Sangill R, Lund TE, et al. Mean diffusional kurtosis in patients with glioma: initial results with a fast imaging method in a clinical setting. AJNR Am J Neuroradiol 2015;36(8):1472–8.
[24] Murakami R, Hirai T, Kitajima M, Fukuoka H, Toya R, Nakamura H, et al. Magnetic resonance imaging of pilocytic astrocytomas: usefulness of the minimum apparent diffusion coefficient (ADC) value for differentiation from high-grade gliomas. Acta Radiol 2008;49(4):462–7.
[25] Cha S. Update on brain tumor imaging: from anatomy to physiology. AJNR Am Neuroradiol 2006;27(3):475–87.
[26] Inglis BA, Bossart EL, Buckley DL, Rd WE, Mareci TH. Visualization of neural tissue water compartments using biexponential diffusion tensor MRI. Magn Reson Med 2001;45(4):580–7.
[27] Li F, Shi W, Wang D, Xu Y, Li H, He J, et al. Evaluation of histopathological changes in the microstructure at the center and periphery of glioma tumors using diffusional kurtosis imaging. Clin Neurol Neurosurg 2016;151:120–7.